JOURNAL OF MATERIALS SCIENCE 27 (1992) 4115–4119

Electrical conductivity of sol–gel derived metal nanoparticles

A. CHATTERJEE, D. CHAKRAVORTY
Indian Association for the Cultivation of Science, Jadavpur, Calcutta-700032, India

Electrically conducting films of thickness ~2 μm have been prepared on ordinary glass slides by growing ultra-fine particles of iron and copper, respectively, from a suitable precursor sol. The diameters of metal particles can be varied from 3–13 nm by controlling the heat-treatment schedule of the sol coating. Resistivity measurements (d.c.) have been carried out over the temperature range 80–300 K. The resistivity values in the range 0.0001–0.0039 Ω cm have been obtained depending on the particle diameter and the type of metal used. The effective Debye temperature θ_D for the different nanoparticle systems have been estimated by fitting the experimental data to the Ziman equation. θ_D is found to vary from 346–408 K for iron with the particle size in the range 3.4–9.5 nm. The values obtained for copper are 243–307 K with particle diameters covering a range of 5.9–12.6 nm.

1. Introduction

The properties of ultra-fine metal particles have been investigated extensively in recent years [1]. Some of these properties include specific heat [2, 3], static polarizability [4–6], magnetic susceptibility [7], photoemission of electrons [8] and optical absorption [9]. While novel behaviour has been shown in the form of enormous photoelectron yield from silver nanoparticles, the expected large value of dielectric permittivity as predicted for an assembly of nanosized metal particles [10] has not been realized so far. Electrical conductivity of small metal particles has also been investigated [11–13]. These measurements have been carried out on vacuum-evaporated metal thin films, the metal particles having diameters > 10 nm. The experimental results have been explained on the basis of a phonon softening effect due to the small size of the metal grains.

Recently we have developed a method of making glass–metal nanocomposites by a sol–gel method [14]. The optical absorption studies reported earlier were carried out on nanocomposites involving iron, cobalt, nickel and manganese, respectively, in a silica glass matrix with the metal phase constituting a volume fraction of only ~ 0.04. We have now prepared samples with the metal phase having a volume fraction large enough for the nanocomposite to exhibit metallic conduction. The electrical conductance of such films has been measured and the results are reported in this paper.

2. Experimental procedure

Nanoparticles of iron and copper have been studied in this work. To prepare the nanocomposites, a precursor sol is firstly made in ethyl alcohol containing silicon tetraethoxide and a suitable salt of the metal concerned. The salts chosen were $FeCl_3$, $6H_2O$ and $Cu(NO_3)_2 \cdot 3H_2O$ for iron and copper, respectively. The sol is made by adding the metal salt and silicon tetraethoxide to a measured volume of ethyl alcohol kept in a glass container. The amounts of the different chemicals used for preparing the sols containing iron and copper, respectively are given in Table I.

Glass slides of dimensions $3 \times 1 \times 0.2$ cm are used for depositing the sols prepared as above. The glass slide is first of all thoroughly cleaned in acetone and dried. The slide is dipped into the sol and then hand-pulled slowly to obtain a coating. The speed of withdrawal is estimated to be 1.5 mm s^{-1}. Several layers could be deposited consecutively by first drying the fresh layer in a laboratory oven at around 100 °C, and then repeating the above procedure. Typically, three such dippings are needed to prepare a 2-μm-thick film. Nanocomposites having different metal particle diameters are made by subjecting the films prepared as above to a reduction treatment in hydrogen at temperatures varying from 450 to 650 °C for periods ranging from 10 min to 1 h. The thicknesses of the films is measured by a Surfometer (Planer Products Ltd, UK). The typical thickness of samples prepared is of the order of 2 μm.

For transmission electron microscopy (TEM), the coatings are scratched off the glass slides by a diamond-tipped cutter and then ground. The powdered samples are dispersed in acetone and then mounted on carbon coated grids. The microstructure and selected area electron diffraction patterns are taken using a JEM 200CX microscope operated at 100 kV. The details of specimen preparation have been described earlier [14].

The d.c. resistivity of the samples containing metal nanoparticles are measured by a conventional four-probe method [11] over the temperature range 80–300 K. Two strips of silver electro dag 1415 (supplied by Acheson Colloiden BV, Holland), painted on

0022–2461

TABLE I Constitution of precursor sols for different nanocomposites.

Metallic species	Inorganic salt	Weight of salt (g)	Volume of silicon tetraethoxide (cm^3)	Volume of ethyl alcohol (cm^3)
Iron	$FeCl_3 \cdot 6H_2O$	11.0	1.0	10.0
Copper	$Cu(NO_3)_2 \cdot 3H_2O$	9.5	1.0	10.0

the conducting surface of the film at a separation of ~ 1 mm, act as the voltage terminals. The end surfaces of the samples are silver painted which act as current terminals.

3. Results

Fig. 1a is an electron micrograph of a nanocomposite containing iron which has been reduced at 650 °C for 1 h; Fig. 1b is the selected area electron diffraction pattern obtained from Fig. 1a. Fig. 2a and b shows the electron micrograph and the selected area electron diffraction pattern for a nanocomposite containing copper which has been reduced at 460 °C for 10 min. These are typical of the micrographs of all other samples. Table II shows the typical d_{hkl} values obtained from nanocomposites containing iron and copper, respectively. The standard ASTM d_{hkl} values for these metals are also given in this table. The agreement between the experimental and standard d_{hkl} values is reasonable. In the case of the Fe/SiO_2 composite, the values 0.2274 and 0.1558 nm correspond to γ-Fe_2O_3 and Fe_3O_4, respectively. The corresponding standard values are 0.2230 and 0.1614 nm. The resistivity data reported below show, however, that these oxide particles do not influence the electrical properties of the composites.

Fig. 3 gives the particle-size distribution in the sample whose micrograph is shown in Fig. 2a. We have fitted the experimental data with a log-normal distribution function:

$$\Delta n = \frac{1}{(2\pi^{1/2})\ln\sigma} \exp\left[-\frac{1}{2}\left\{\frac{\ln\left(\frac{x}{\bar{x}}\right)}{\ln\sigma}\right\}^2\right] \Delta(\ln x) \quad (1)$$

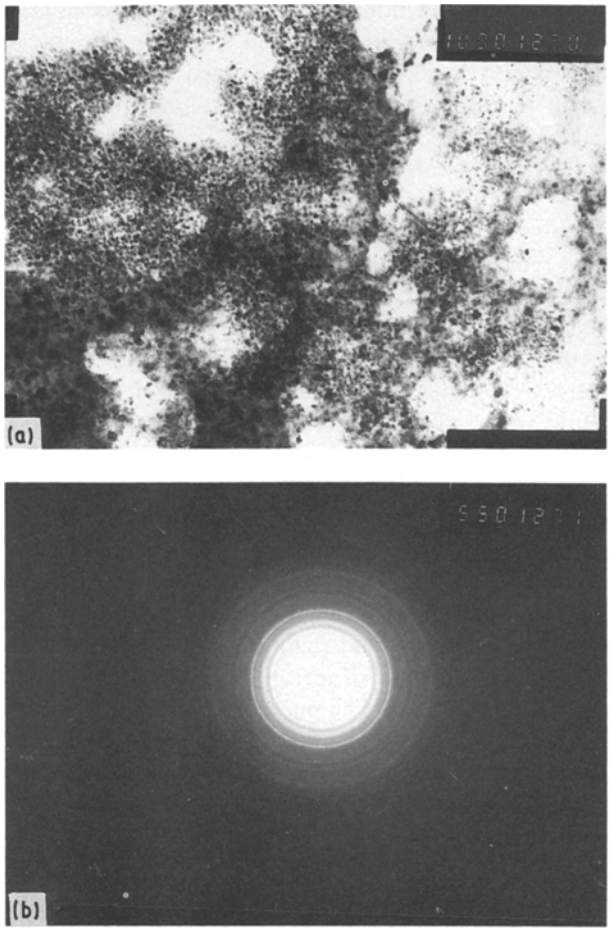

Figure 1 (a) EM of Fe/SiO_2 composite reduced at 650 °C for 1 h. (b) Electron diffraction pattern of (a).

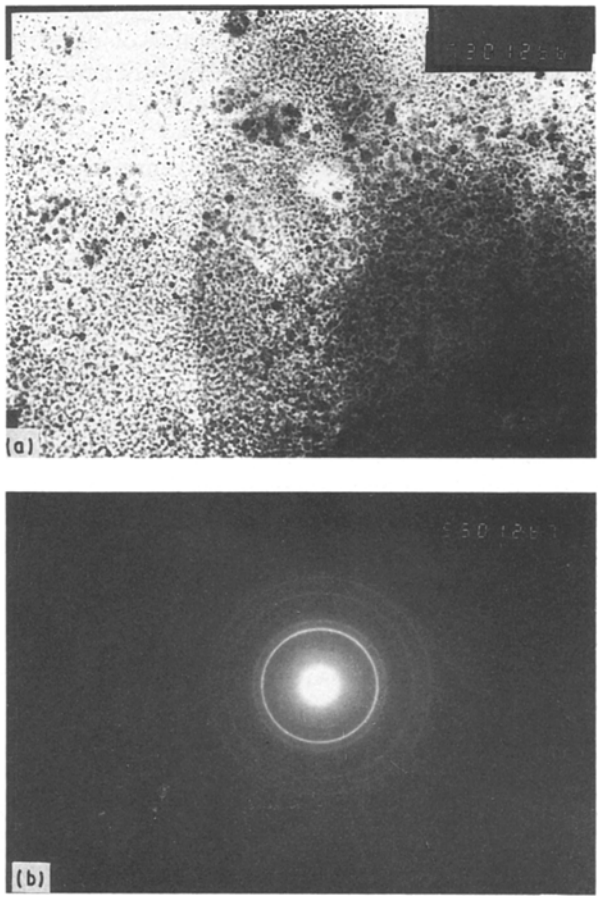

Figure 2 (a) EM of Cu/SiO_2 composite reduced at 460 °C for 10 min. (b) Electron diffraction pattern of (a).

TABLE II Comparison of d_{hkl} values (nm) obtained from electron diffractogram data of different nanocomposites with standard ASTM values.

Fe/SiO_2		Cu/SiO_2	
Observed	Standard iron	Observed	Standard copper
0.2274		0.2061	0.2088
0.2013	0.2026	0.1805	0.1808
0.1558		0.1245	0.1278
0.1421	0.1433		0.109
0.1203	0.1170	0.1062	0.104
0.1110	0.1013	0.0903	0.0903

TABLE III Summary of reduction treatment schedule and particle diameters for different nanocomposites.

Composite	Reduction treatment	$\bar{x}$ (nm)	Log-normal distribution, σ
Fe/SiO_2	530 °C, 15 min	3.4	1.2
	550 °C, 35 min	5.6	1.3
	600 °C, 25 min	8.3	1.2
	650 °C, 1 h	9.5	1.3
Cu/SiO_2	460 °C, 10 min	5.9	1.2
	500 °C, 15 min	7.8	1.2
	500 °C, 45 min	10.5	1.2
	550 °C, 30 min	12.6	1.2

where Δn is the fractional number of particles; x is the diameter; $\bar{x}$ is the median diameter; and σ is the geometric standard deviation. The solid line in Fig. 3 represents the least-square fitted distribution function with the values of median diameter $\bar{x}$ and the geometric standard deviation given in the figure caption. Table III summarizes these values for samples subjected to different reduction treatments.

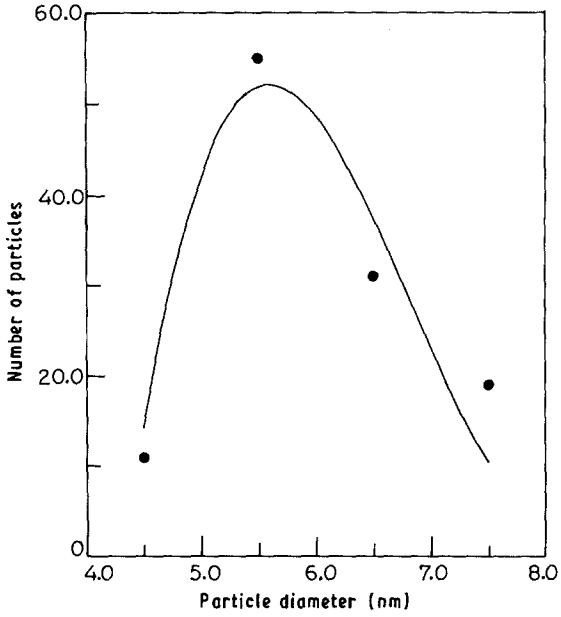

Figure 3 Particle-size distribution in Figure 2a. Points, experimental data; line, theoretical curve drawn from Equation 1 with $\bar{x} = 5.9$ nm and $\sigma = 1.2$.

Fig. 4 shows the resistivity variation as a function of temperature for various samples containing iron nanoparticles of different diameters. Fig. 5 gives the temperature dependence of resistivity for samples containing copper particles. It is evident that the resistivity varies linearly over the temperature range

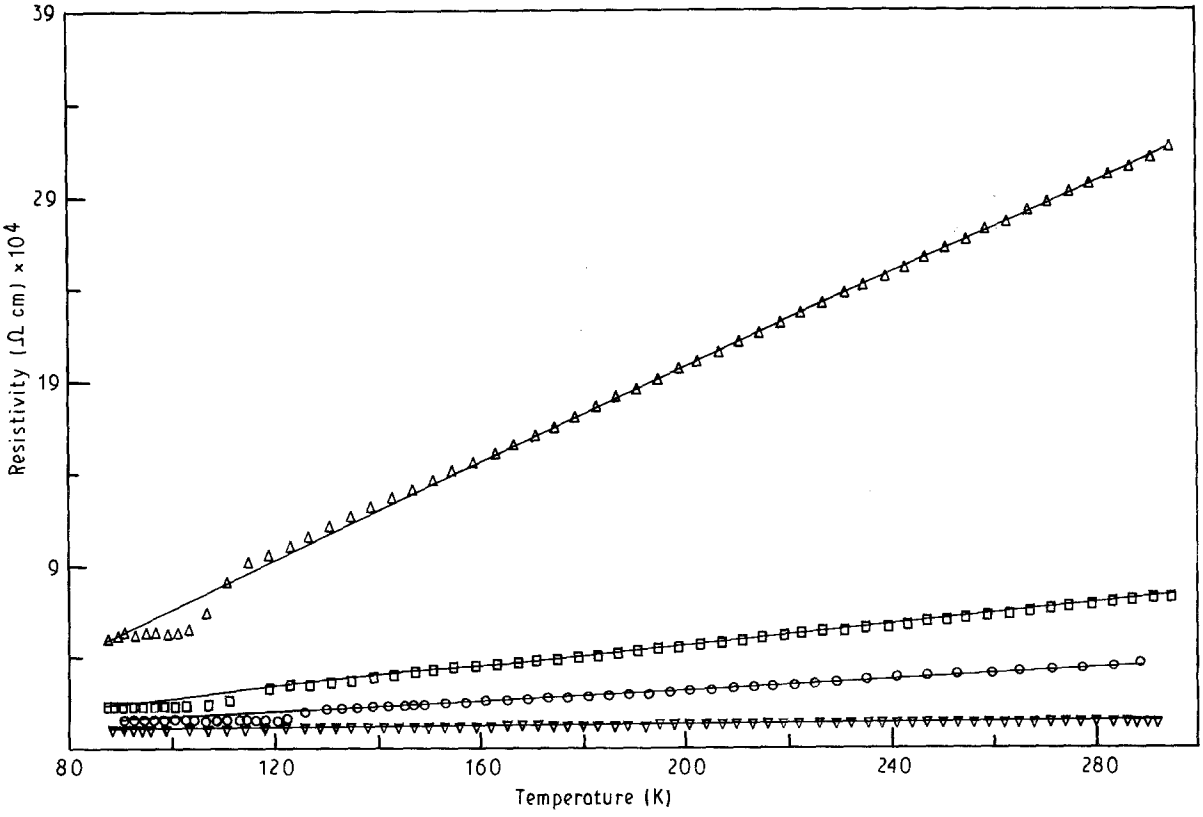

Figure 4 Resistivity variation as a function of temperature for different Fe/SiO_2 nanocomposites. △, 3.4; □, 5.6; ○, 8.3; ▽ 9.3 nm.

TABLE IV θ_D and C values for different nanocomposites.

Composite	Particle diameter (nm)	θ_D (K)	ρ_0 (Ω cm)	C (Ω cm K)
Fe/SiO_2	9.5	408	0.01×10^{-5}	0.1
	8.3	390	0.1×10^{-5}	0.8
	5.6	361	0.4×10^{-4}	1.2
	3.4	346	0.01×10^{-3}	4.9
Cu/SiO_2	12.6	307	0.3×10^{-5}	2.0×10^{-2}
	10.5	288	4.2×10^{-5}	9.1×10^{-2}
	7.8	261	0.4×10^{-5}	4.1×10^{-2}
	5.9	243	1.4×104	4.3×10^{-1}

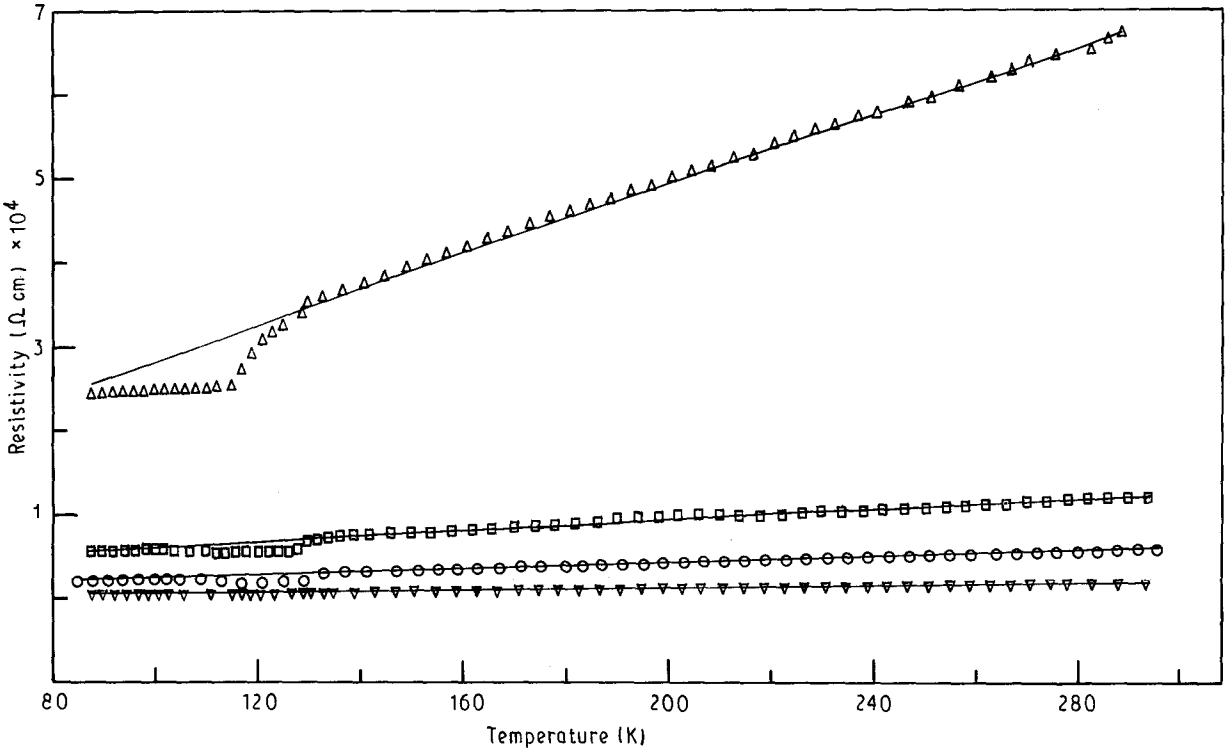

Figure 5 Resistivity variation as a function of temperature for different Cu/SiO_2 nanocomposites. △, 5.9; □, 7.8; ○, 10.5; ▽, 12.6 nm.

130–300 K. Also, the rate of resistivity change increases as the metal particle diameter becomes smaller. A break is observed in the linear variation of resistivity at a temperature around 120 K for both iron and copper. These results are discussed in the next section.

4. Discussion

The electrical resistivity of a bulk metal is given by the Ziman expression [15] as shown below

$$\rho_L = C/\theta_D\,(T/\theta_D)^5 \int_0^{\theta_D/T} z^5\,dz/(e^z - 1)\,(1 - e^{-z}) \tag{2}$$

where ρ_L is the resistivity due to lattice vibrations; θ_D is the Debye temperature; T is the temperature; and C is a constant.

Fujita *et al.* [12] have used Equation 2 to analyse the electrical resistivity data of metallic films of silver and aluminium, respectively, having a particle size in the range 10–30 nm. These authors have studied the effect of particle size on resistivity by treating θ_D as a floating parameter. We have followed a similar procedure to investigate the effect of metal particle diameter on electrical conductivity, though our experimental data are limited to the temperature range 80–300 K. We find that even under this limitation there is a systematic variation of θ_D with a particle diameter of the two metallic species.

The experimental resistivity data have been fitted to Equation 2 using C and θ_D as parameters. We find that the experimental results match an equation of the form

$$\rho = \rho_0 + \rho_L \tag{3}$$

where ρ_0 is a constant.

In Figs 4 and 5 the solid lines represent the least-square fitted curves as obtained by the above procedure.

Table IV summarizes the values of C, θ_D and ρ_0 for iron and copper particles, respectively, with different diameters. As indicated in this table the effective Debye temperature is found to decrease as the metal

particle diameter is reduced. This is consistent with a softening of the phonon spectrum due to the effect of the surface of the metallic particles. The trend of the present data as shown by Equation 3 is also consistent with Mathiesson's rule [11]. The value of the constant C decreases with an increase in the size of the metallic particles. As mentioned earlier, larger particles are formed after an enhanced reduction treatment. The latter also brings about the formation of a larger number of percolation chains comprising metal particles. The lowering of the value of C is therefore believed to arise due to a decrease in the overall resistance of the films containing larger particles.

The temperature-independent term ρ_0 is thought to arise due to some defects – either point or line – within the metal grains. It has not been possible, however, to draw conclusions about the exact nature of defects from the present data.

The breaks in the linear plots of resistivity against temperature as shown in Figs 4 and 5 are believed to arise due to the morphology of metal clusters in different specimens. A likely model is the presence of a multi-fractal configuration of the chain-like metal clusters contributing to metallic conduction in the present nanocomposite system [16]. The model visualizes the existence of regions within the metallic chains which have a fractal dimension larger than that of the rest of the chain length. At lower temperatures, these regions control the rate of change of resistivity as a function of temperature. As a result a discontinuity in the slope of the resistivity–temperature plot is observed. However, detailed EM studies of the metal clusters and delineation of their fractal dimensions are necessary to substantiate the above model. Such work is now in progress.

In conclusion, a novel technique has been developed to prepare films of nanoparticles of iron and copper, respectively, by a sol–gel route with particle diameters ranging from 3–13 nm. The films show a wide range of resistivities, the latter depending on the metal particle diameter.

Acknowledgments

This work was supported by the Department of Science and Technology, Government of India. Electron microscopy was carried out at RSIC, Bose Institute, Calcutta.

References

1. H. P. BALTES and E. SIMANEK, "Aerosol Microphysics II" edited by W. H. Marlow (Springer, Berlin, 1982) p. 7.
2. V. NOVOTNY and P. P. M. MEINCKE, *Phys. Rev.* **B8** (1973) 4168.
3. G. H. COMSA, D. HEITKAMP and H. S. RADE, *Solid State Commun.* **24** (1977) 547.
4. F. MEIER and P. WYDER, *Phys. Lett.* **A39** (1972) 51.
5. R. DUPREE and M. A. SMITHARD, *J. Phys. C: Solid State Phys.* **5** (1972) 408.
6. S. STRASSLER and M. J. RICE, *Phys. Rev.* **B6** (1972) 2575.
7. R. A. BUHRMAN and W. P. HALPERIN, *Phys. Rev. Lett.* **30** (1973) 692.
8. A. SCHMITT-OTT, P. SCHURTENBERGER and H. C. SIEGMAN, *ibid.* **45** (1980) 1284.
9. A. ANDERSON. O. HUNDERI and C. G. GRANQVIST, *J. Appl. Phys.* **57** (1980) 757.
10. L. P. GORKOV and G. M. ELIASHBERG, *Zh. Eksp. Teor. Fiz.* **48** (1965) 1407.
11. T. FUJITA, K. OHSHIMA and N. WADA, *J. Phys. Soc. Jpn* **27** (1969) 1459.
12. T. FUJITA, K. OHSHIMA and T. KUROISHI, *ibid.* **40** (1976) 90.
13. K. OHSHIMA, T. FUJITA and T. KUROISHI, *J. Phys. Paris (Cologne)* **38** (1977) C2-163.
14. A. CHATTERJEE and D. CHAKRAVORTY, *J. Phys. D: Appl. Phys.* **22** (1989) 1386.
15. J. M. ZIMAN, "Electrons and Phonons" (Clarendon, Oxford, 1960) p. 364.
16. B. ROY and D. CHAKRAVORTY, *J. Phys.: Condens Matter.* **2** (1990) 9323.

Received 4 April
and accepted 30 July 1991